

ROLE OF ANOMALOUS CHROMOMAGNETIC INTERACTION IN POMERON AND ODDERON STRUCTURES AND IN GLUON DISTRIBUTION

*N. Kochelev*¹

Joint Institute for Nuclear Research, Dubna

We calculate the contribution arising from nonperturbative quark–gluon chromomagnetic interaction to the high-energy total quark–quark cross section and to gluon distributions in nucleon. The estimation obtained within the instanton model of QCD vacuum leads to the conclusion that this type of interaction gives the dominating contribution to the Pomeron coupling with the light quarks and to gluon distribution in light hadrons at small virtualities of quarks and gluons. We argue that the Odderon, which is the $P = C = -1$ partner of the Pomeron, is governed by the spin-flip component related to nonperturbative three-gluon exchange induced by anomalous quark–gluon chromomagnetic interaction.

Вычислен вклад непертурбативного хромомангнитного кварк-глюонного взаимодействия в полное сечение рассеяния кварков при высоких энергиях и в распределение глюонов в нуклоне. Оценка, полученная в инстантонной модели вакуума КХД, приводит к заключению, что это взаимодействие дает основной вклад в константу взаимодействия померона с легкими кварками и в распределение глюонов в легких адронах при малых виртуальностях кварков и глюонов. Приводятся аргументы, что оддерон, партнер померона с $P = C = -1$, возникает из амплитуды с переворотом спина, связанной с обменом тремя глюонами за счет аномального кварк-глюонного хромомангнитного взаимодействия.

PACS: 24.85.+p

INTRODUCTION

The gluon distribution in nucleon is one of the central quantities in particle physics which determines the high-energy cross section values of the huge amount of important processes. In spite of the tremendous achievements in the last years in the measurement of this distribution, full understanding of the dynamics of gluons inside hadrons is absent so far (see [1, 2]). In the Regge theory the behaviour of the gluon distribution function at small Bjorken x is controlled by the contribution coming from the Pomeron exchange which may have the so-called «soft» and «hard» parts [3]. Usually, the hard Pomeron is associated with the perturbative BFKL regime [4] and the soft part is assumed to be originated from nonperturbative QCD dynamics [5]. Nonperturbative effects arise from the complex structure of QCD vacuum. The instantons are one of the well-studied topological fluctuations of vacuum

¹E-mail: kochelev@theor.jinr.ru

gluon fields which might be responsible for many nonperturbative phenomena observed in particle physics (see [6, 7]). Their possible importance in the structure of the Pomeron and gluon distribution was considered in quite different approaches [7–11] for the different approximations to the complicated quark–gluon dynamics in instanton vacuum. In particular, it was shown [12] that instantons lead to the appearance of anomalous chromomagnetic quark–gluon interaction (ACQGI). It was demonstrated that this new type of quark–gluon interaction might be responsible for the observed large single-spin asymmetries in various high-energy reactions [12, 13]. Furthermore, it gives a large contribution to the high-energy quark–quark scattering cross section [14]. The first estimation of the effect of ACQGI on nucleon gluon distribution was made in [8] and small x behavior $g(x) \propto 1/x$ corresponding to the soft Pomeron was found. It was clear from that study that anomalous chromomagnetic interaction should also play an important role in the structure of the Pomeron. Indeed, recently the model for the soft Pomeron based on this interaction has been suggested [7].

In this paper, we consider the detailed structure of the Pomeron and gluon distribution with the special attention to the interplay between their perturbative and nonperturbative components. We also discuss the possible manifestation of ACQGI in the Odderon exchange.

1. ANOMALOUS CHROMOMAGNETIC QUARK–GLUON INTERACTION

In the general case, the interaction vertex of massive quark with gluon can be written in the following form:

$$V_\mu(k_1^2, k_2^2, q^2)t^a = -g_s t^a \left[\gamma_\mu F_1(k_1^2, k_2^2, q^2) - \frac{\sigma_{\mu\nu} q_\nu}{2M_q} F_2(k_1^2, k_2^2, q^2) \right], \quad (1)$$

where the form factors $F_{1,2}$ describe nonlocality of the interaction, $k_{1,2}$ is the momentum of incoming and outgoing quarks, respectively, and $q = k_1 - k_2$, M_q is the quark mass, and $\sigma_{\mu\nu} = (\gamma_\mu \gamma_\nu - \gamma_\nu \gamma_\mu)/2$. In various applications to high-energy reactions based on perturbative QCD (pQCD) it is usually assumed that only nonspin-flip first term in Eq. (1) (Fig. 1, *a*) contributes and one can neglect the second term in this equation, Fig. 1, *b*, because in the limit of the massless quark this term should be absent due to quark chirality conservation in massless pQCD. However, it has recently been shown that such an assumption has no justification in nonperturbative QCD and the second term might give in many cases even a dominant contribution to high-energy reactions in comparison with the first one [12, 14].

The cornerstone of this phenomenon is the spontaneous chiral symmetry breaking (SCSB) due to the complex topological structure of the QCD vacuum. Indeed, the instanton liquid

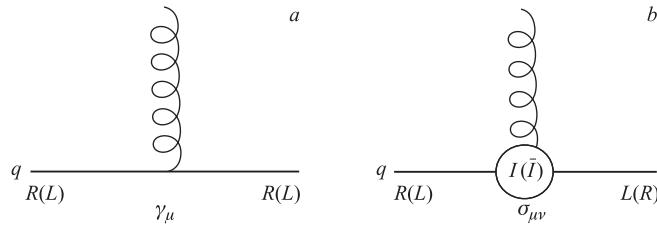


Fig. 1. The quark–gluon coupling: *a*) perturbative; *b*) nonperturbative. Symbols R and L denote quark chirality and symbol $I(\bar{I})$ denotes instanton (antiinstanton)

model for QCD vacuum [6, 7] provides the mechanism for such a breaking. That mechanism is related to the existence of quark-zero modes in the instanton field. As a result of SCSB, the light quarks in nonperturbative QCD vacuum have the dynamical mass, M_q . Additionally, 't Hooft quark–quark interaction induced by quark-zero modes leads to the violation of $U(1)_A$ symmetry in strong interaction.

In high-energy reactions one might naively expect the smallness of SCSB effects because of the energy $\sqrt{s} \gg M_q$. Indeed, it might be correct for the reactions where the dominating contribution comes from quark-exchange diagrams. Within the instanton model this type of diagrams is originated from the 't Hooft quark–quark interaction contribution. However, instantons also lead to specific *quark–gluon chromomagnetic interaction* [12] which is presented by the second term in Eq. (1) (Fig. 1, b). It is evident that this term should lead to a non-vanishing contribution to high-energy reactions because it induces t -channel nonperturbative gluon exchange. The size of the contribution is determined by the value of anomalous quark chromomagnetic moment (AQCM)¹

$$\mu_a = F_2(0, 0, 0). \quad (2)$$

We should point out that within the instanton model the shape of form factor $F_2(k_1^2, k_2^2, q^2)$ is fixed:

$$F_2(k_1^2, k_2^2, q^2) = \mu_a \Phi_q(|k_1| \rho/2) \Phi_q(|k_2| \rho/2) F_g(|q| \rho), \quad (3)$$

where

$$\begin{aligned} \Phi_q(z) &= -z \frac{d}{dz} (I_0(z) K_0(z) - I_1(z) K_1(z)), \\ F_g(z) &= \frac{4}{z^2} - 2K_2(z) \end{aligned} \quad (4)$$

are the Fourier-transformed quark-zero mode and instanton fields, respectively, and $I_\nu(z)$, $K_\nu(z)$ are the modified Bessel functions and ρ is the instanton size.

The value of AQCM is determined by the effective density of the instantons $n(\rho)$ in nonperturbative QCD vacuum [12]:

$$\mu_a = -\pi^3 \int \frac{d\rho n(\rho) \rho^4}{\alpha_s(\rho)}. \quad (5)$$

The shape of instanton density in the form

$$n(\rho) = n_c \delta(\rho - \rho_c) \quad (6)$$

leads to AQCM which is proportional to the packing fraction of instantons $f = \pi^2 n_c \rho_c^4$ in vacuum

$$\mu_a = -\frac{\pi f}{\alpha_s(\rho_c)}. \quad (7)$$

¹The definition of AQCM used in Eq. (2) differs by a factor of two from the corresponding quantity presented in [12] and [7].

By using the following relation between parameters of the instanton model [15]

$$f = \frac{3}{4}(M_q \rho_c)^2, \quad (8)$$

we obtain

$$\mu_a = -\frac{3\pi(M_q \rho_c)^2}{4\alpha_s(\rho_c)}. \quad (9)$$

This formula coincides with the result for AQCM presented in Eq.(7.2) in the paper by Diakonov [7] and shows the direct connection between AQCM and SCSB phenomena. The dimensionless parameter $\delta = (M_q \rho_c)^2$ is one of the main parameters of the instanton model. It is proportional to the packing fraction of instantons in QCD vacuum $\delta \propto f \ll 1$, Eq. (8), and is rather small. For a fixed value of average instanton size $\rho_c^{-1} = 0.6$ GeV it changes from $\delta^{\text{MF}} = 0.08$ for $M_q = 170$ MeV in the mean field approximation [6] to $\delta^{\text{DP}} = 0.33$ for $M_q = 345$ MeV within Diakonov–Petrov model (DP) [16]. For the strong coupling constant at the scale of instanton average size [6,7]

$$\alpha_s(\rho_c) \approx 0.5, \quad (10)$$

we obtain the following values for AQCM:

$$\mu_a^{\text{MF}} \approx -0.4, \quad \mu_a^{\text{DP}} \approx -1.6 \quad (11)$$

in the mean field approximation and in the DP approach, respectively. We would like to emphasize that in spite of the strong dependence of AQCM on the value of the effective quark mass in QCD vacuum, AQCM is very large in the wide interval of the possible changing of instanton model parameters. The origin of this peculiarity is in the large numerical factor in front of δ in Eq. (9) for AQCM. Indeed, this formula can be rewritten in the following form:

$$\mu_a = -\frac{3}{8}S_0\delta, \quad (12)$$

where $S_0 = 2\pi/\alpha_s(\rho)$ is the Euclidean instanton action. The typical value of this action is very large [6,7]

$$S_0 \approx 10-15, \quad (13)$$

and leads to the compensation of the δ smallness effect on AQCM.

Within the instanton model approach the first term in Eq. (1) is related to the nonzero mode contribution to quark propagator in the instanton field. The nonzero modes contribution to quark propagator can be approximated with high accuracy by perturbative propagator [6]. Due to zero mode dominance for the light quarks [6], we can expect that for the light quarks this sort of contribution should be suppressed in comparison with the second term in Eq. (1). However, for heavy quark the first term should dominate because there are no zero modes for heavy quark in the instanton field. Furthermore, instanton induced form factors in the chromomagnetic part of interaction suppress the contribution of the second term for highly virtual quark and/or gluon. Therefore, form factor in the first term in Eq. (1) might be chosen in the form

$$F_1(k_1^2, k_2^2, q^2) = \Theta(|k_1^2| - \mu^2)\Theta(|k_2^2| - \mu^2)\Theta(|q^2| - \mu^2), \quad (14)$$

where μ is the factorization scale between perturbative and nonperturbative regimes. In our estimation below we will use $\mu \approx 1/\rho_c \approx 0.6$ GeV.

2. FINE POMERON STRUCTURE

Let us estimate the contribution of the vertex, Eq. (1), to the total high-energy quark–quark scattering cross section. The leading diagrams contributing to the nonspin-flip amplitude of q – q scattering are shown in Fig. 2 and for colorless t -channel exchange present the model of the Pomeron. The imaginary part of the total forward scattering amplitude gives the total quark–quark cross section.

So, in our model the Pomeron includes the pure perturbative exchange (Fig. 2, *a*), nonperturbative (Fig. 2, *c*) diagrams and the mixed graph (Fig. 2, *b*).

By using the relation, Eq. (9), the total contribution to quark–quark cross section for the quarks with small virtualities is

$$\sigma^{\text{tot}} = \sigma^{\text{pert}} + \sigma^{\text{mix}} + \sigma^{\text{nonpert}}, \quad (15)$$

where

$$\sigma^i = \int_{q_{\text{min}}^2}^{\infty} \frac{d\sigma^i(t)}{dt} dq^2, \quad (16)$$

$$\frac{d\sigma(t)^{\text{pert}}}{dt} = \frac{8\pi\alpha_s^2(q^2)}{9q^4}, \quad \frac{d\sigma(t)^{\text{mix}}}{dt} = \frac{\alpha_s(q^2)\pi^2 |\mu_a| \rho_c^2 F_g^2(|q|\rho_c)}{3q^2}, \quad (17)$$

$$\frac{d\sigma(t)^{\text{nonpert}}}{dt} = \frac{\pi^3 \mu_a^2 \rho_c^4 F_g^4(|q|\rho_c)}{32},$$

where $q^2 = -t$ and $q_{\text{min}}^2 \approx 1/\rho_c^2$ for perturbative and mixed contributions, and $q_{\text{min}}^2 = 0$ for pure nonperturbative (Fig. 2, *c*) contribution.

For the strong coupling constant, the following parametrization was used for the case $N_f = 3$:

$$\alpha_s(q^2) = \frac{4\pi}{9 \ln((q^2 + m_g^2)/\Lambda_{\text{QCD}}^2)}, \quad (18)$$

where $\Lambda_{\text{QCD}} = 0.280$ GeV and the value $m_g = 0.88$ GeV was fixed from the requirement $\alpha_s(q^2 = 1/\rho_c^2) \approx \pi/6$ [7]. This form describes the frozen coupling constant in the infrared region, $\alpha_s(q^2) \rightarrow \text{const}$ as $q^2 \rightarrow 0$.

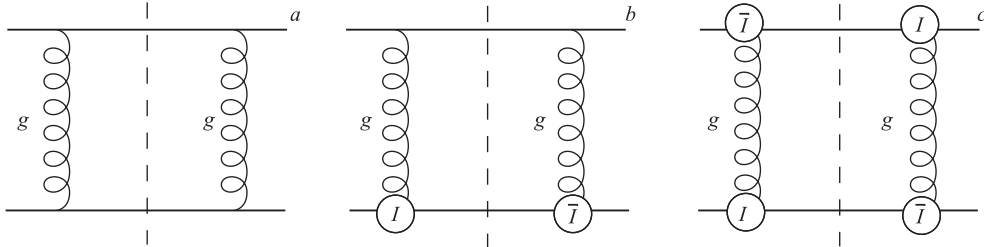


Fig. 2. The fine Pomeron structure in the model with perturbative interaction and nonperturbative ACQGI: *a*) perturbative contribution; *b*) interference perturbative and nonperturbative vertices; *c*) nonperturbative contribution. The symbol I (\bar{I}) denotes instanton (antiinstanton)

The result of calculation of the different contributions to the total quark–quark scattering cross section is presented in Fig.3 as a function of AQCM. It is evident that within the interval $0.4 < |\mu_a| < 1.6$ the main contribution comes from the terms related to the anomalous quark–gluon chromomagnetic interaction. Recently, the effects of nonzero AQCM in hadron spectroscopy have been considered (see [17] and references therein). It was shown that the value of

$$\mu_a = -1 \quad (19)$$

is favoring to describe the fine structure of hadron spectrum. This value of AQCM corresponds to dynamical quark mass $M_q = 280$ MeV. This mass is in agreement with recent result of analysis of dressed-quark propagator within DSE approach involving the lattice-QCD data from [21]. We will adopt this value in our estimations below. For that set of parameters the total quark–quark cross section $\sigma_{qq}^{\text{tot}} = 3.05$ mb is the sum of the following partial cross sections:

$$\sigma_{qq}^{\text{pert}} = 0.63 \text{ mb}, \quad \sigma_{qq}^{\text{mix}} = 1.22 \text{ mb}, \quad \sigma_{qq}^{\text{nonpert}} = 1.21 \text{ mb}, \quad (20)$$

and it is not far away from «experimental» quark constituent model value $\sigma_{qq}^{\text{exp}} \approx 4$ mb, which is needed to describe the inelastic proton–proton and proton–antiproton cross sections; $\sigma_{PP(\bar{P})}^{\text{in}} = 36$ mb in the energy range where they are approximately constant. One may expect also an additional contribution to the total cross section arises from the multigluon and multiquark emission induced by the quark–gluon–instanton vertex. It will bring our estimation to the experimental value. It follows from Eq.(20) that the contribution to the quark–quark cross section due to nonperturbative chromomagnetic quark–gluon interaction is about 80% and the contribution from pure perturbative exchange is about 20% and quite small. Therefore, within our model the dynamics of the soft Pomeron is determined not by the γ_μ -like quark–gluon vertex (Fig. 1, *a*) as in most conventional models for the Pomeron, but by the $\sigma_{\mu\nu}$ vertex pictured in Fig. 1, *b*. The widely assuming statement is that the difference in the dynamics of soft and hard Pomerons comes from the difference in their dependence on such kinematic variables as total energy and transfer momenta. From our point of view, the main source of difference between two exchanges arises from a completely different spin structure of quark–gluon interaction inside the Pomeron exchange.

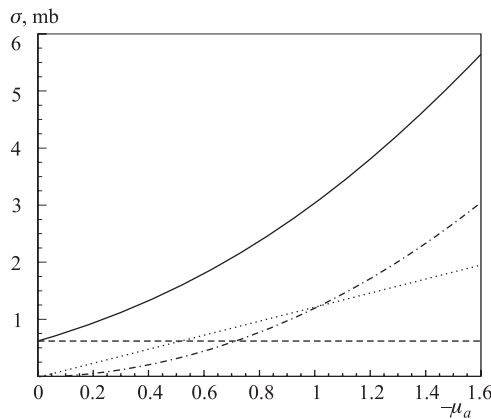


Fig. 3. The contribution to the total quark–quark cross section as a function of AQCM: perturbative (dashed line), mixed (dotted line), nonperturbative (dash-dotted line) and their sum (solid line)

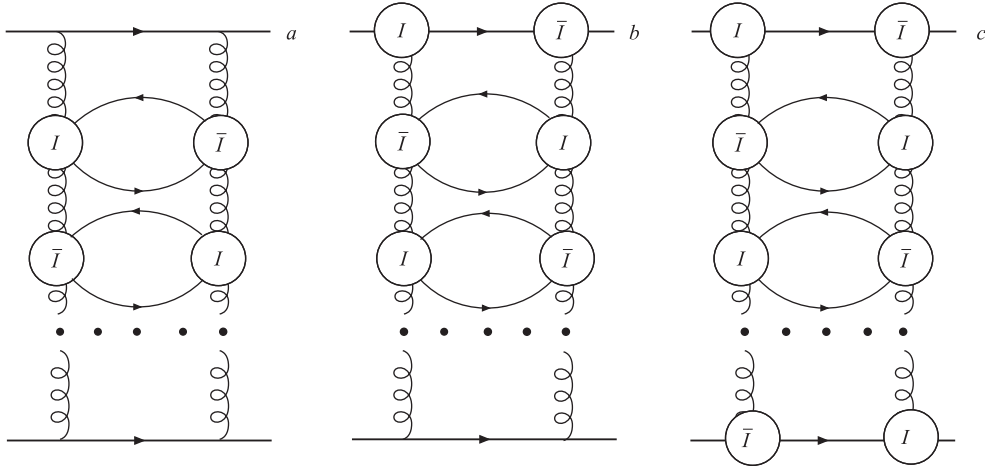


Fig. 4. The example of the diagrams which give the contribution to energy-dependent part of the Pomeron exchange

In the above estimation only the simplest contributions to the Pomeron exchange presented in Fig. 2 were considered. Due to pure spin-one t -channel exchange they lead to cross section independent of the energy. Therefore, the effective Pomeron intercepts $\alpha_P = 1$ in this approximation. It is well known that the experimental data show that the value of the soft Pomeron intercepts $\alpha_P(0) \approx 1.08$ [22]. In spite of the fact that empirically the soft Pomeron intercepts close to one, its deviation from one leads to visible energy dependence of the total and diffractive cross sections and to a large subleading contributions at very high energies. Some of diagrams which provide such subleading contributions in our model are presented in Fig. 4. It is evident that at low energy such contributions should be suppressed by even powers of small packing fraction of instantons in QCD vacuum, $f^n < 1/4^n, n = 2, 4, \dots$. However, due to their logarithmic growth with increasing of energy they might give the dominant contribution at very large energy. The calculation of these contributions is beyond this paper and will be the subject of the separate publication [23].

3. CHROMOMAGNETIC ODDERON

Within the conventional approach, the Odderon $P = C = -1$ partner of the Pomeron, originates from three-gluon exchange (Fig. 5, *a*) with nonspin-flip perturbative-like quark-gluon vertex [24–28]. The experimental support of the existence of such an exchange comes from high-energy ISR data on the difference in the dip structure around $|t| \approx 1.4$ GeV between the proton–proton and proton–antiproton differential cross sections [18]. However, there is no any signal for the Odderon at very small transfer momentum t [19].

According to our model, the perturbative part of the Odderon, Fig. 5, *a*, in the region of momentum transfer $|t|/9 \leq 1/\rho_c^2$ is expected to be much smaller in comparison with the nonperturbative part presented by the graphs, Fig. 5, *b, c*¹.

¹The detailed calculation will be published elsewhere.

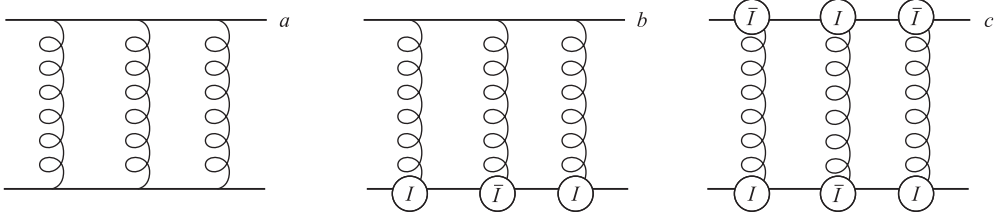


Fig. 5. The structure of the Odderon exchange: *a*) nonspin-flip perturbative three-gluon exchange; *b*, *c*) nonperturbative spin-flip contributions

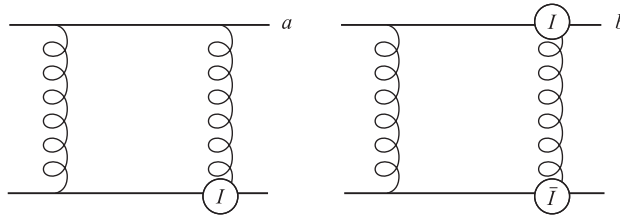


Fig. 6. The example of the diagrams which give the contribution to spin-flip component of the Pomeron

It is clear that the first diagram gives rise to the nonspin-flip amplitude of quark–quark scattering, the diagram in Fig. 5, *b* leads to single spin-flip and the diagram in Fig. 5, *c* presents double spin-flip (see helicity structure of vertices in Fig. 1). By using the conventional notation for helicity amplitudes $\Phi_n = \langle \lambda_{i_1} \lambda_{i_2} | \lambda_{f_1} \lambda_{f_2} \rangle$ (see, e.g., [20]), where $n = 1, \dots, 5$ and $\lambda_{i_{1,2}(f_{1,2})}$ are helicities of initial (final) quarks, respectively, one can see that the graph in Fig. 5, *a* gives the contribution to the Φ_1 and Φ_3 amplitudes, diagram in Fig. 5, *b* contributes to the Φ_5 amplitude, and Fig. 5, *c* gives rise to the Φ_4 amplitude. Our conjecture is that the spin-flip amplitude dominates in the Odderon exchange. Therefore, one might expect that the Odderon should strongly interfere with the spin-flip part of the Pomeron. Some of the diagrams which give rise to the spin-flip part of the Pomeron are presented in Fig. 6.

We would like to mention that in [29–31] an alternative mechanism for the spin-flip component of the Pomeron and the Odderon [29] was discussed. This mechanism is based on the existence of the quark–diquark component in the nucleon wave function.

4. GLUON DISTRIBUTION AND CHROMOMAGNETIC QUARK–GLUON INTERACTION

It was shown above that the Pomeron structure is rather complicated. It includes perturbative, «hard», and nonperturbative, «soft», parts and their interference, «soft-hard» part.

Therefore, this structure should also manifest itself in the structure of gluon distribution in nucleon. One of the ways to show it is in the use of a DGLAP-like approach [32,33] with the modified quark splitting function \mathcal{P}_{Gq} according to the vertex, Eq. (1) [8]. The diagrams giving the contribution to nucleon gluon distribution in our model are presented in Fig. 7.

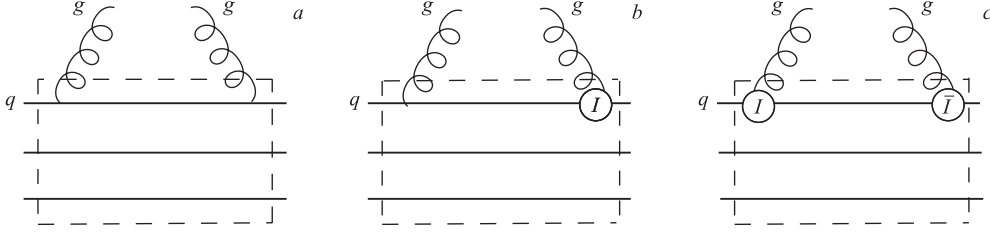


Fig. 7. The diagrams contributing to nucleon gluon distribution: a) «hard»-perturbative; b) «hard-soft» interference perturbative and nonperturbative exchanges; c) «soft»-nonperturbative part

At present, unintegrated gluon distribution is widely used in different applications (see, for example, [34,35]). To calculate this distribution, we use the convolution model formula

$$f(x, k_{\perp}^2) = N_q k_{\perp}^2 \int_x^1 \frac{dy}{y} \mathcal{P}_{Gq} \left(\frac{x}{y}, k_{\perp}^2 \right) q_V(y), \quad (21)$$

where $N_q = 3$ is the number of valence quarks in nucleon; q_V is the valence quark distribution function in nucleon; \mathcal{P}_{Gq} is the quark splitting function as defined in [33], and we neglect possible intrinsic momentum dependence of q_V related to the confinement scale.

The splitting function for the general vertex Eq. (1) is given by the formula

$$\mathcal{P}_{Gq}(z, k_{\perp}^2) = \frac{C_F z(1-z)k_{\perp}^2}{8\pi^2(k_{\perp}^2 + M_q^2 z^2)^2} \sum_{\lambda} \text{Tr} \left\{ (\hat{k}_C + M_q) U_{\mu}(t) (\hat{k}_A + M_q) \bar{U}_{\rho}(t) \right\} \epsilon_{\mu}(\lambda) \epsilon_{\rho}^*(\lambda), \quad (22)$$

where $U_{\mu}(t) = V_{\mu}(0, 0, t)$, k_A (k_C) is momentum of initial (final) quark, $t = q^2 = (k_A - k_C)^2$, $\bar{U} = \gamma_0 U^{\dagger} \gamma_0$ and λ is gluon helicity. In the infinite momentum frame

$$\begin{aligned} k_A &= \left(P, P + \frac{M_q^2}{2P}, \mathbf{0}_{\perp} \right), \\ k_C &= \left((1-z)P + \frac{k_{\perp}^2 + M_q^2}{2(1-z)P}, (1-z)P, -\mathbf{k}_{\perp} \right), \\ q &= \left(zP - \frac{k_{\perp}^2 + M_q^2 z}{2(1-z)P}, zP, \mathbf{k}_{\perp} \right), \end{aligned} \quad (23)$$

the result for splitting function is

$$\begin{aligned} \mathcal{P}_{Gq}(z, k_{\perp}^2) &= \frac{C_F k_{\perp}^2}{2\pi z(k_{\perp}^2 + M_q^2 z^2)^2} \left[(\sqrt{\alpha_s(|t|)} \Theta(|t| - \Lambda^2) + \sqrt{\alpha_s(1/\rho_c^2)} \mu_a \times \right. \\ &\quad \left. \times F_g(|t|)^2 z^2 + 2((1-z)\alpha_s(|t|) \Theta(|t| - \Lambda^2) + \frac{\alpha_s(1/\rho_c^2) \mu_a^2 k_{\perp}^2}{4M_q^2} F_g^2(|t|)) \right], \end{aligned} \quad (24)$$

where $|t| = (k_{\perp}^2 + M_q^2 z^2)/(1-z)$ is the gluon virtuality in Fig. 7.

The integrated distribution is given by

$$g(x, Q^2) = \int_0^{Q^2} \frac{dk_{\perp}^2}{k_{\perp}^2} f(x, k_{\perp}^2). \quad (25)$$

For estimation we use a simple form for valence quark distribution

$$q_V(x) = 1.09 \frac{(1-x)^3}{\sqrt{x}} \quad (26)$$

with the normalization

$$\int_0^1 q_V(x) dx = 1. \quad (27)$$

The result of calculation of unintegrated gluon distribution at $x = 10^{-2}$ is presented in Fig. 8 as a function of k_{\perp}^2 . The result for integrated gluon distribution at small $Q^2 = 1 \text{ GeV}^2$ is pictured in Fig. 9. It is evident that the nonperturbative contribution dominates in both unintegrated and integrated gluon distributions. For the large Q^2 perturbative contribution starts to dominate due to its stronger Q^2 dependence. Such a difference in the Q^2 dependence is directly related to the difference in the k_{\perp}^2 behavior between perturbative and nonperturbative contributions coming from the nonspin-flip and spin-flip part of the general quark–gluon vertex, Eq. (1). In Fig. 9 we also present the comparison of our result with some available phenomenological parametrizations. By taking into account the uncertainties in the extraction of gluon distribution from the data and our simple parametrization for valence quark distribution we may say that agreement is rather good.

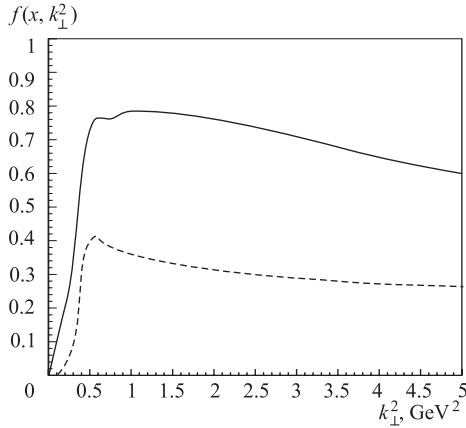


Fig. 8. The unintegrated gluon distribution at $x = 10^{-2}$: solid (dashed) line is total (perturbative) contribution

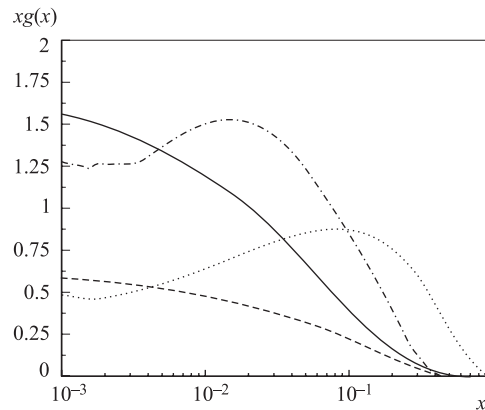


Fig. 9. Perturbative (dashed line) and total (solid line) contributions to gluon distribution at $Q^2 = 1 \text{ GeV}^2$ in comparison with some of the phenomenological fits: dotted line is ALEKHIN02LO set and dash-dotted line is MSTW2008LO fit [36]

CONCLUSION

In summary, we suggest a new approach to the Pomeron and Odderon structures and gluon distribution in hadrons. It is based on the modified quark–gluon vertex which includes the nonperturbative spin-flip part related to anomalous chromomagnetic interaction. It is shown that this interaction gives the main contribution to the Pomeron coupling to small virtuality light quarks and to the gluon distribution in nucleon. Our conjecture is that the origin of the difference between «soft» and «hard» Pomerons is related to the difference in the spin structure of quark–gluon interaction governing these effective exchanges. We give the arguments in favor of the spin-flip dominance in the Odderon exchange.

Acknowledgements. The author is very grateful to I. O. Cherednikov, A. E. Dorokhov, S. V. Goloskokov, E. A. Kuraev, N. N. Nikolaev, and L. N. Lipatov for useful discussions. This work was supported in part by RFBR grant 10-02-00368-a, by Belarus–JINR grant, and by Heisenberg–Landau program.

REFERENCES

1. *Landshoff P. V.* Fundamental Problems with Hadronic and Leptonic Interactions. hep-ph/0903.1523.
2. *Ivanov I. P., Nikolaev N. N., Savin A. A.* Diffractive Vector Meson Production at HERA: From Soft to Hard QCD // *Part. Nucl.* 2006. V. 37. P. 1; hep-ph/0501034.
3. *Landshoff P. V.* Soft and Hard QCD. hep-ph/0209364.
4. *Kuraev E. A., Lipatov L. N., Fadin V. S.* The Pomeranchuk Singularity in Non-Abelian Gauge Theories // *Sov. Phys. JETP.* 1977. V. 45. P. 199; *ZhETF.* 1977. V. 72. P. 377;
Balitsky I. I., Lipatov L. N. The Pomeranchuk Singularity in Quantum Chromodynamics // *Sov. J. Nucl. Phys.* 1978. V. 28. P. 822; *Yad. Fiz.* 1978. V. 28. P. 1597;
Lipatov L. N. The Bare Pomeron in Quantum Chromodynamics // *Sov. Phys. JETP.* 1986. V. 63. P. 904; *ZhETF.* 1986. V. 90. P. 1536.
5. *Landshoff P. V., Nachtmann O.* Vacuum Structure and Diffraction Scattering // *Z. Phys. C.* 1987. V. 35. P. 405.
6. *Schäfer T., Shuryak E. V.* // *Rev. Mod. Phys.* 1998. V. 70. P. 1323.
7. *Diakonov D.* // *Prog. Part. Nucl. Phys.* 2003. V. 51. P. 173.
8. *Kochelev N. I.* Instanton Contribution to Polarized and Unpolarized Gluon Distributions in Nucleon. hep-ph/9707418.
9. *Shuryak E. V., Zahed I.* Instanton-Induced Effects in QCD High-Energy Scattering // *Phys. Rev. D.* 2000. V. 62. P. 085014.
10. *Kharzeev D. E., Kovchegov Y. V., Levin E.* QCD Instantons and the Soft Pomeron // *Nucl. Phys. A.* 2001. V. 690. P. 621.
11. *Dorokhov A. E., Cherednikov I. O.* Instanton Effects in Quark Form Factor and Quark–Quark Scattering at High Energy // *Ann. Phys.* 2004. V. 314. P. 321.
12. *Kochelev N. I.* // *Phys. Lett. B.* 1998. V. 426. P. 149.

13. *Cherednikov I. O. et al.* Instanton Contribution to the Sivers Function // Phys. Lett. B. 2006. V. 642. P. 39.
14. *Kochelev N.* Soft Contribution to Quark–Quark Scattering Induced by an Anomalous Chromomagnetic Interaction // JETP Lett. 2006. V. 83. P. 527.
15. *Dorokhov A. E., Kochelev N. I., Esaibegian S. V.* Multi-Instanton Contribution to QCD Sum Rules for the Nucleon and Pion // Phys. At. Nucl. 1996. V. 59. P. 2006; Yad. Fiz. 1996. V. 59. P. 2081.
16. *Diakonov D., Petrov V. Y.* A Theory of Light Quarks in the Instanton Vacuum // Nucl. Phys. B. 1986. V. 272. P. 457.
17. *Ebert D., Faustov R. N., Galkin V. O.* Mass Spectra and Regge Trajectories of Light Mesons in the Relativistic Quark Model. hep-ph/0903.5183.
18. *Breakstone A. et al.* A Measurement of Anti- PP and PP Elastic Scattering in the Dip Region at $S^{**}(1/2) = 53$ GeV // Phys. Rev. Lett. 1985. V. 54. P. 2180.
19. *Landshoff P. V., Nachtmann O.* Some Remarks on the Pomeron and the Odderon in Theory and Experiment. hep-ph/9808233.
20. *Bourrely C., Soffer J., Leader E.* Polarization Phenomena in Hadronic Reactions // Phys. Rep. 1980. V. 59. P. 95.
21. *Bhagwat M. S., Tandy P. C.* Analysis of Full-QCD and Quenched-QCD Lattice Propagators // AIP Conf. Proc. 2006. V. 842. P. 225; nucl-th/0601020.
22. *Donnachie A., Landshoff P. V.* Total Cross Sections // Phys. Lett. B. 1992. V. 296. P. 227.
23. *Kochelev N.* To be published.
24. *Gauron P., Nicolescu B., Leader E.* // Nucl. Phys. B. 1988. V. 299. P. 640.
25. *Donnachie A., Landshoff P. V.* The Coupling of the Odderon // Nucl. Phys. B. 1991. V. 348. P. 297.
26. *Bartels J., Lipatov L. N., Vacca G. P.* A New Odderon Solution in Perturbative QCD // Phys. Lett. B. 2000. V. 477. P. 178.
27. *Ewerz C.* The Odderon in Quantum Chromodynamics. hep-ph/0306137.
28. *Braun M. A.* Odderon with a Running Coupling Constant // Eur. Phys. J. C. 2008. V. 53. P. 59.
29. *Zakharov B. G.* // Sov. J. Nucl. Phys. 1989. V. 49. P. 860; Yad. Fiz. 1989. V. 49. P. 1386.
30. *Kopeliovich B. Z., Zakharov B. G.* Spin-Flip Component of the Pomeron // Phys. Lett. B. 1989. V. 226. P. 156.
31. *Goloskokov S. V., Kuleshov S. P., Selyugin O. V.* // Z. Phys. C. 1991. V. 50. P. 455;
Goloskokov S. V. // Phys. Lett. B. 1993. V. 315. P. 459;
Goloskokov S. V., Kroll P. // Phys. Rev. D. 1999. V. 60. P. 014019.
32. *Dokshitzer Y. L.* Calculation of the Structure Functions for Deep Inelastic Scattering and e^+e^- Annihilation by Perturbation Theory in Quantum Chromodynamics // Sov. Phys. JETP. 1977. V. 46. P. 641; ZhETF. 1977. V. 73. P. 1216;
Gribov V. N., Lipatov L. N. Deep Inelastic ep Scattering in Perturbation Theory // Sov. J. Nucl. Phys. 1972. V. 15. P. 438; Yad. Fiz. 1972. V. 15. P. 781.

548 *Kochelev N.*

33. *Altarelli G., Parisi G.* // Nucl. Phys. B. 1977. V. 126. P. 298.
34. *Kimber M. A., Martin A. D., Ryskin M. G.* Unintegrated Parton Distributions // Phys. Rev. D. 2001. V. 63. P. 114027.
35. *Ivanov I. P., Nikolaev N. N.* // Phys. Rev. D. 2002. V. 65. P. 054004.
36. <http://www-spires.dur.ac.uk/hepdata/pdf3.html>

Received on February 18, 2010.